Synthesis and Characterization of an Iron(II) Bipyridine Redox-Active Polymer

Adolfo I. B. Romo, Joaquín Rodríguez-López*

Department of Chemistry and Beckman Institute for Advance Science and Technology, University of Illinois Urbana-Champaign, 600 South Matthew Ave., Urbana, Illinois 61801, USA.

ABSTRACT

Soluble redox-active polymers (RAPs) are promising materials for energy storage applications in redox flow batteries. Here, we present the synthesis and characterization of a new metal-based Redox-Active Polymer (RAP) based on iron(II) bipyridine pendants and a modified polyvinyl benzyl chloride (PVBC) as backbone structure. Our metallopolymer called Fe-RAP was characterized by Fourier transform infrared spectroscopy (FTIR), inductively coupled plasma optical emission spectroscopy (ICP-OES), ultraviolet-visible spectroscopy (UV-Vis) and dynamic light scattering (DLS). FTIR results showed the disappearance of the -CH_2-Cl band at 1264 cm^{-1}, and subsequent appearance of a quaternary salt due the insertion of $(CH_3)_2$N-phen, later to be modified for redox activity with [Fe(Cl_2)($Bpy)_2$]. ICP suggested that about 75% of the available sites of the original PVBC backbone were modified with Fe. Electronic spectra in the UV-Vis region reinforce the presence of Fe(II) metallocentre in the polymer due the charge-transfer metal-to-ligand (MLCT) in 520nm. Finally, DLS showed that the polymer is free of small molecules or precursors. Cyclic voltammetry at an ultramicroelectrode showed redox activity at 0.6 V vs Fc^+.

INTRODUCTION

Redesigned battery concepts are needed to keep up with societal energy demands. Redox flow batteries (RFBs) are emerging as attractive solutions for energy storage due to their ability to level the inherently intermittent nature of solar and wind energy.[1-3] These batteries use electrolytic solutions with soluble redox species which allow for power and energy to be scaled independently, in contrast to Li-ion batteries.[4] The state-of-the-art RFB is the partially commercialized aqueous vanadium system, whose deployment has suffered from the high cost of this metal, expensive cell membranes, and low storage energy density.[5] One way to address all three of these drawbacks is with the use of Redox Active Polymers (RAPs) since their bulky size enables the use of inexpensive cell membranes like CELGARD or PIMs.[6-10] In such a size-exclusion redox flow battery, charge-storing, bulky polymers are prevented from crossing-over through a nanoporous separator, enabling the operation of the battery with stable and inexpensive polyelectrolytes.[10] Herein, we present the synthesis and characterization of a new Iron(II) bipyridine redox active polymer (Fe-RAPs) for potential applications in RFBs that was characterized by FTIR, ICP, UV-Vis, and DLS.

EXPERIMENTAL SECTION

Chemicals. Iron(II) chloride tetrahydrate, 2,2'-bipyridine and 1,10-phenanthroline-5-amine were purchased from Sigma Aldrich (St. Louis, MO). Methanol, methylene chloride, acetonitrile, dimethylformamide, diethyl ether, acetone, formic acid and formaldehyde were purchased from Fisher Chemical. Unsubstituted polymer backbone, poly(4-vinyl benzyl chloride) MW: 112 KDa was purchased from Polymer Source.

Synthetic procedures.

The synthetic procedure and the structures of Fe-RAPs are presented in Scheme 1. We used a stepwise synthesis to first prepare a PVB-phen backbone from commercial PVBC and phenanthroline, and then promote the reaction of $[Fe(Cl_2)(Bpy)_2]$ with the PVB-phen backbone to yield the desired polymer, **Scheme 1**. The metallic precursor $[Fe^{II}(bpy)_2Cl_2]$ was characterized by routine ESI mass spectroscopy, while the metallopolymer was characterized by FTIR, ICP, UV-Vis, and DLS as described below.

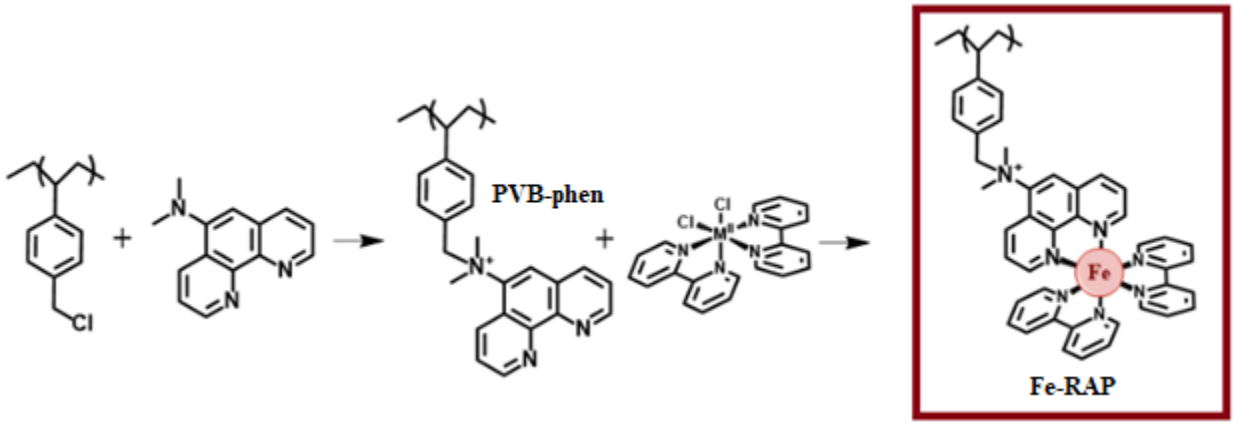

Scheme 1. Schematical representation of the chemical structures of precursors, synthetic route of Fe-RAPs. Estimative number of pendants based in the ICP on average of Fe-RAP 479 pendants.

N,N-dimethyl-1,10-phenanthrolin-4-amine ($(CH_3)_2$N-phen). The synthesis of the ligand was adapted from the methylation of an aniline.[11] 1,10-phenanthroline-5-amine (0.5 g, 2.5 mmol) was added to formic acid (0.575 g, 12.5 mmol) in an ice bath and stirred for 30 minutes. Formaldehyde (0.165 g, 5.5 mmol) was added to the mixture and was refluxed for 2 hours. The mixture reacted overnight under reflux and subsequently was rotavaporated to remove excess formic acid and formaldehyde. Finally, the solid was washed with dry ethyl ether to remove water. Yield 90%. 1H-NMR (Chloroform-d, 500 MHz) δ: 9.21 (d, J = 4.4, 1.7 Hz, 1H), 9.07 (d, J = 4.3, 1.6 Hz, 1H), 8.94 (d, J = 8.3, 1.7 Hz, 1H), 8.37 (s, 1H), 7.81 (dd, J = 8.3, 4.4 Hz, 1H), 7.56 (dd, J = 8.3, 4.3 Hz, 1H),

5.24 (s, 3H) and 4.76 (s, 3H). ESI mass spectra m/z: 222.08 ($C_{14}H_{12}N_3^+$), calculated 222.10 ($C_{13}H_{16}N_3^+$).

Poly(4-vynil-benzyl-N-phen) (PVB-phen). The synthesis of the ligand was adapted from the a previously reported procedure for making a viologen polymer.[12] Dry DMF (15 mL) was added to a flask containing PVBC (0.05 g, 0.33 mmol) and $(CH_3)_2$N-phen (0.36 g, 3.27 mmol) under nitrogen atmosphere. The reaction mixture was stirred at 90 ºC for 6 days. Saturated solution of NH_4PF_6 solution was prepared in water and added to the above reaction mixture. The resultant solution was stirred at room temperature for 12 h. The precipitated polymer was centrifugated and washed with diethyl ether three times. PVB-phen was dried under vacuum for 48 h. The polymer was not soluble in any deuterated solvent to perform NMR characterization. ATR-IR $\nu_{(>N+<)}$ at 1601 cm^{-1} was observed.

[Fe(bpy)Cl₂]. The complex was prepared according to literature with a little modification on synthetic procedure.[13] Were added 15 mL of a 2-propanol solution containing $FeCl_2$*$4H_2O$ (0.95 g, 0.15 mol) on 135 mL of 2-propanol solution containing 2,2'- bipyridine (2.125g, 0.005 mol). The reaction mixture was continuously stirred 6 h at 30 ºC. It was cooled with ice bath and fine crystalline material containing $[Fe(byp)_2Cl_2]$ complex was then filtered. This was subsequently washed with cold 2-propanol and diethyl ether

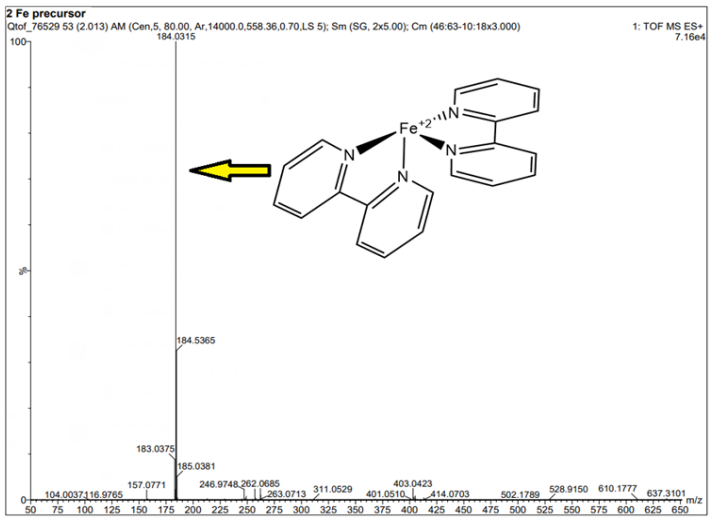

Figure 1. High resolution ESI mass spectra for $[Fe(bpy)_2Cl_2]$.

solution to eliminate impurities. The yield of the crystalline dark red material was 71%. (ESI positive mode) m/z: 184.0315 ($[Ru(bpy)_2]^{2+}$) = ($C_{20}H_{16}FeN_4^{2+}$). (Figure 1).

Redox Active Poly(4-vynil-benzyl-N-phen-Fe^{II}-$(bpy)_2$) (Fe-RAPs). We added 0.001 mol of Fe bipyridine precursor ($[Fe(bpy)_2Cl_2]$) to a suspension of PVB-phen (0.356 g, 0.001 mol) in 50 mL of methanol. The mixture was stirred under reflux for 6 hours, and subsequently was cooled to room temperature. Saturated aqueous solution of NH_4PF_6 was added on the mixture observing a fluffy precipitate, the solution was stirred for 2 hour and let rest for 30 minutes in an ice bath. The precipitate was centrifugated at 15.000 rpm for 10 minutes. The aqueous solution was removed and the solid was redissolved in acetonitrile, reprecipitated with 40 mL of NH_4PF_6 and was centrifugated. The solid product was dried under vacuum for 1 day. Subsequently, a chromatographic column was made using sephadex LH-20 as the stationary phase and acetonitrile as the mobile phase. The small particles were retained in the gel and the first fraction was collected as a polymer free of metal precursors.

Fe-RAP. (Red wine powder, Yield 48%), $\nu_{(>N+<)}$ 1602 cm^{-1}, UV-Vis MLCT in 481 nm (ε = 6.948) and 520 nm (ε = 8292), elemental analysis for Fe by ICP showed ~75% of site modification (~479 Fe pendants per average polymer coil).

Apparatus. High-resolution ESI measurements were made with a Waters Q-TOF Ultima ESI equipment. Solid state infrared spectra were recorded using a PerkinElmer Frontier ATR-IR spectrophotometer equipped with a KRS5 thallium bromine/iodide Universal Attenuated Total Reflectance accessory. The UV-Vis experiments were performed on Shimadzu UV-2501PC UV-Vis spectrometer with quartz cuvette. The ICP date was collected at Microanalysis Lab at the School of Chemical science at the University of Illinois at Urbana-Champaign. Hydrodynamic

radius of the M-RAPs 5 mM in acetonitrile was evaluated spectroscopically via dynamic light scattering (DLS) using a Malvern Zetasizer Nano. Samples were passed through a 0.2 μm syringe filter (Cole Parmer) to remove dust contaminants and aggregates. Calculated hydrodynamic radii are presented as Z-averages arising from fits of the cumulants of the autocorrelation function. Cyclic voltammetry experiments in a three-electrode configuration were carried out inside an Ar-filled drybox and a CHI 940D potentiostat was used.

RESULT AND DISCUSSION

The PVB-phen was modified with an excess addition of $[Fe^{II}(bpy)_2Cl_2]$. The Fe-RAP was characterized using DLS, ATR-IR, UV−vis absorption spectra, and ICP. It was not possible get ^1H NMR characterization due the traces of Fe^{III} paramagnetism in the samples.

DLS experiments (Figure 2) show that the polymers are free of small molecules, corresponding to the metallic precursors. It was also possible to observe the presence of large molecules corresponding to aggregates of the polymers. However, after passing through a 200 nm filter, they changed size, generating smaller subunits in 40 nm of hydrodynamic radius, which correspond to Fe-RAPs without aggregation. Is important highlight that it was not was possible to observe smaller molecules such as $[Fe(Cl)_2(bpy)_2]$ precursors.

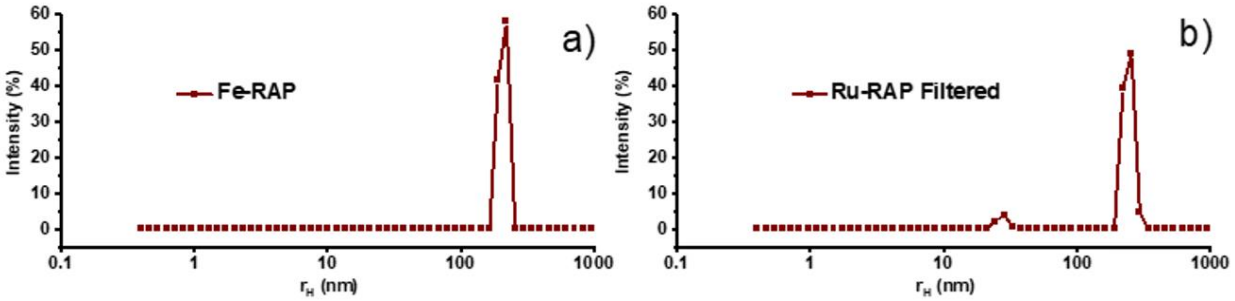

Figure 2. DLS measurements of an acetonitrile solution containing 5 mM of Fe-RAP before (a) and after syringe filtering (b).

ATR-IR spectra (Figure 3) of PVBC showed a characteristic νCH_2Cl stretching appears at 1280 cm^{-1}, corresponding to the pendants fragments of the monomer in the non-modified polymer. After insertion of the phenanthroline fragment into PVBC (PVB-phen), the band at 1280 cm^{-1} disappears and a new band emerges at 1601 cm^{-1}, this peak corresponding to quaternary amine ($\nu>N^{+}<$). For Fe-RAPs this band is maintained after the addition of the metal fragment, which shows the stability of the system and confirms the insertion of phenanthroline fragment. Additionally, was possible to observe the C=C and C=N stretching and vibration of bipyridine and phenanthroline rings around 1430 cm^{-1}.

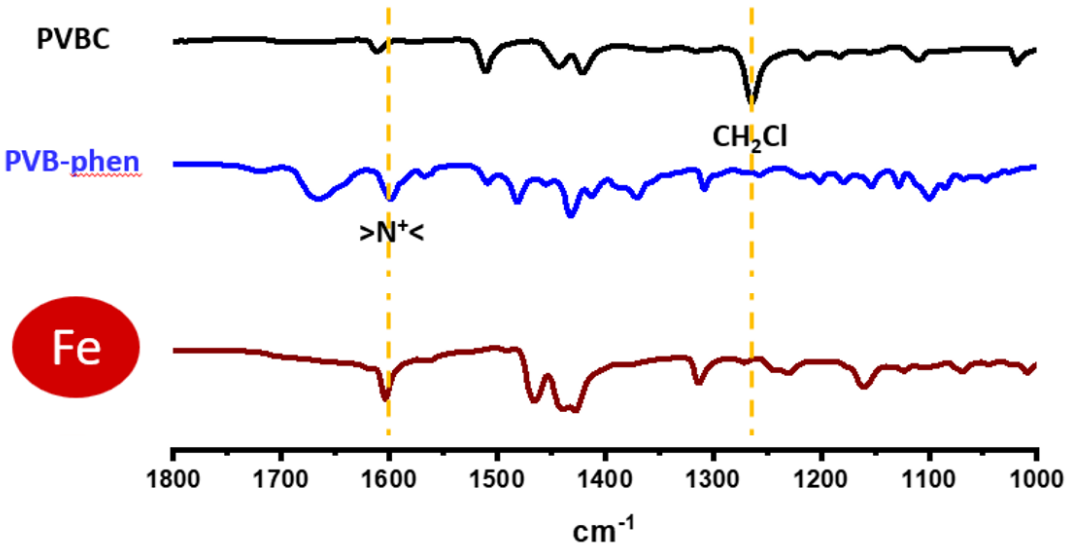

Figure 3. ATR-IR spectra for PVBC (black), PVB-phen (blue), Fe-RAP (brown).

Electronic spectra in the UV-Vis region (Figure 4) showed two different absorption band for the Metal to Ligand Charge-Transfer (MLCT) for Fe-RAP in 481 and 520 nm with molar extinction coefficient of 6948 and 8292 $M^{-1}cm^{-1}$ respectively. Additionally, it was possible observe the intraligand electronic transitions in the organic fragment of the polymer under 350 nm.

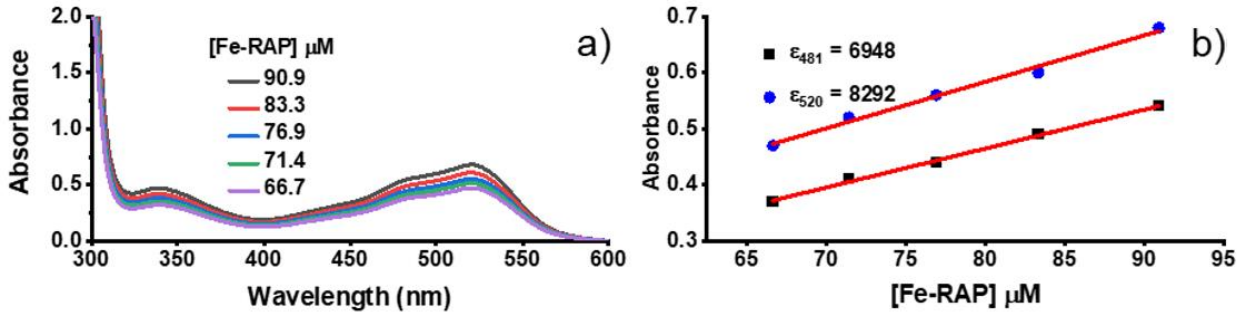

Figure 4. Electronic spectra UV-Vis in acetonitrile solution containing Fe-RAP (a), and plot of a Fe-RAP at different concentration vs absorbance in b).

Similar behavior was observed for several Fe bipyridine and phenanthroline derivates when the oxidation state of metallocentre is Fe(II).[14-16] The MLCT generated around 500 nm are commonly found in $[Fe(bpy)_3]^{2+}$ or $[Fe(phen)_3]^{2+}$ complexes. Interestingly, as was well reported, Fe(III) complexes shown lability of the ligand coordinated to metallocentre. This property enables the polymer to generate cross-links.

The amount of metal present in the Fe-RAP was calculated using ICP (Table 1). We used as base the 644 CH_2-Cl fragments present in the commercial polymer of 112 kDa before modifications. We determined based on the percentage of Fe detected in the ICP experiments that we have 479 atoms of iron in each average polymer chain. Fe-RAP showed 74.4% of Fe(II) fragment insertion in the polymeric structure. The partial modification is likely due to the bulky size of the metallocenter compared to the anchoring site in the main chain of the polymer. In addition, due to the lability of the metal centers, it is possible that a chelate effect occurs, with the phenanthroline fragments of the polymer, removing some bipyridine ligands. However, the percentage of modification of the polymers is greater than 75%. Additionally, it was not possible to observe small structures for the Fe precursor in the DLS measurements (Figure 2).

Table 1. Polymer Fe insertion percentage and number of pendants determined by ICP.

M-RAPs	Calculated (%)	Founded (%)	Difference	Modification (%)	Number of Pendants
Fe-RAP	4.70	3.5	-1.20	74	479

Finally, redox activity was tested via cyclic voltammetry (CV), as shown in Figure 5. CV experiments were conducted in a solution of 1 mM of Fe-RAP in acetonitrile using 0.1 M $TBAPF_6$ as supporting electrolyte and a scan rate of 1 mV/s. The working electrode was a 25-micrometer diameter Pt ultramicroelectrode (UME) probe and a Ag^+/Ag quasireference electrode was used, but the potential later calibrated to the ferrocene scale and reported as vs. Fc^+/Fc. The resulting voltammogram shows a clear sigmoidal redox wave – which is characteristic for UME voltammetry – centered around 0.6 V vs. Fc^+/Fc, different from the precursors $[Fe(bpy)_2Cl_2]$ (0.25 V vs. Fc^+/Fc) and $FeCl_2$ (0.04 V vs. Fc^+/Fc). This Fe-RAP potential is consistent with the expected potential for Fe polypyridyl complexes. The CV curve reaches a steady-state mass transfer limited current, indicating fast electrode kinetics, and thus, potential for its use in a high-energy density redox flow battery.

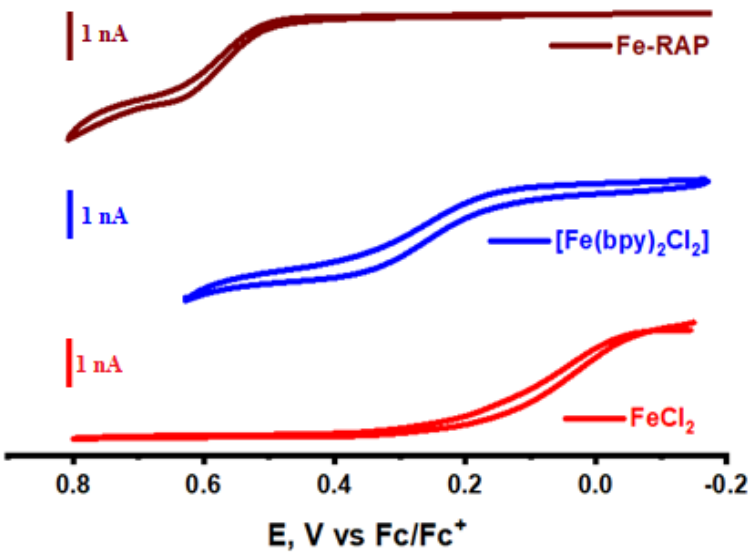

Figure 5. Cyclic voltammetry of acetonitrile solution containing 0.1 M of $TBAPF_6$ and $1x10^{-3}$ M of Fe-RAP (wine), $[Fe(bpy)_2Cl_2]$ (blue), and $FeCl_2$ (red).

CONCLUSION

In this study, we synthesized and characterized a new iron(II) bipyridine Redox-Active Polymer (Fe-RAP) derived from polyvinyl benzylic backbone. The new polymer was well characterized by DLS, FTIR, UV-Vis, and ICP. FTIR results showed the disappearance of the -CH_2-Cl band in 1264 cm^{-1}, and consecutive appearance of a quaternary salt due to the insertion of $(CH_3)_2$N-phen and [Fe(Cl_2)($Bpy)_2$] fragment. This fact confirms the insertion of an iron pendant in the backbone polymer. Additionally, ICP suggested that the polymer was modified in about 75% of its backbone. We determined that Fe-RAP has 479 pendants based on the average size of the coil of the commercial PVBC. Electronic spectra in the UV-Vis region reinforce the presence of Fe(II) metallocentre in the polymer due the charge-transfer metal-to-ligand (MLCT) observed at 520 nm. DLS showed that the polymer is free of small molecules or precursors. Finally, CV characterization of the Fe-RAP in acetonitrile shows a redox potential of ~0.6 V vs Fc^+/Fc and fast kinetics, making this a candidate for testing in redox flow batteries. We consider Fe-RAP as a jumpstart in the design of new polyelectrolytes, and surely, we will see similar polymers using other metals.

Conflict of interest

The authors declare no conflict.

ACKNOWLEDGMENT

The research was financially supported by the Joint Center for Energy Storage Research (JCESR), an Energy Innovation Hub funded by the U.S. Department of Energy, Office of Science, Basic Energy Sciences.

References

1. Schubert, C.; Hassen, W. F.; Poisl, B.; Seitz, S.; Schubert, J.; Usabiaga, E. O.; Gaudo, P. M.; Pettinger, K.-H. Hybrid Energy Storage Systems Based on Redox-Flow Batteries: Recent Developments, Challenges, and Future Perspectives *Batteries* [Online], 2023.
2. Sinclair, N. S.; Savinell, R. F.; Wainright, J. S., A perspective on the design and scale up of a novel redox flow battery. *MRS Energy & Sustainability* **2022,** *9* (2), 387-391.
3. Tang, L.; Leung, P.; Xu, Q.; Mohamed, M. R.; Dai, S.; Zhu, X.; Flox, C.; Shah, A. A., Future perspective on redox flow batteries: aqueous versus nonaqueous electrolytes. *Current Opinion in Chemical Engineering* **2022,** *37*, 100833.
4. Tian, G.; Yuan, G.; Aleksandrov, A.; Zhang, T.; Li, Z.; Fathollahi-Fard, A. M.; Ivanov, M., Recycling of spent Lithium-ion Batteries: A comprehensive review for identification of main challenges and future research trends. *Sustainable Energy Technologies and Assessments* **2022,** *53*, 102447.
5. Lee, S.; Kim, M.; Park, J.; Choi, J.; Kang, J.; Park, M., A High Voltage Aqueous Zinc–Vanadium Redox Flow Battery with Bimodal Tin and Copper Clusters by a Continuous-Flow Electrometallic Synthesis. *ACS Applied Materials & Interfaces* **2023,** *15* (5), 7002-7013.
6. Burgess, M.; Chénard, E.; Hernández-Burgos, K.; Nagarjuna, G.; Assary, R. S.; Hui, J.; Moore, J. S.; Rodríguez-López, J., Impact of Backbone Tether Length and Structure on the Electrochemical Performance of Viologen Redox Active Polymers. *Chemistry of Materials* **2016,** *28* (20), 7362-7374.
7. Burgess, M.; Hernández-Burgos, K.; Schuh, J. K.; Davila, J.; Montoto, E. C.; Ewoldt, R. H.; Rodríguez-López, J., Modulation of the Electrochemical Reactivity of Solubilized Redox Active Polymers via Polyelectrolyte Dynamics. *Journal of the American Chemical Society* **2018,** *140* (6), 2093-2104.
8. Burgess, M.; Moore, J. S.; Rodríguez-López, J., Redox Active Polymers as Soluble Nanomaterials for Energy Storage. *Accounts of Chemical Research* **2016,** *49* (11), 2649-2657.
9. Montoto, E. C.; Cao, Y.; Hernández-Burgos, K.; Sevov, C. S.; Braten, M. N.; Helms, B. A.; Moore, J. S.; Rodríguez-López, J., Effect of the Backbone Tether on the Electrochemical Properties of Soluble Cyclopropenium Redox-Active Polymers. *Macromolecules* **2018,** *51* (10), 3539-3546.
10. Montoto, E. C.; Nagarjuna, G.; Moore, J. S.; Rodríguez-López, J., Redox Active Polymers for Non-Aqueous Redox Flow Batteries: Validation of the Size-Exclusion Approach. *Journal of The Electrochemical Society* **2017,** *164* (7), A1688.
11. Clarke, H. T.; Gillespie, H. B.; Weisshaus, S. Z., The Action of Formaldehyde on Amines and Amino Acids1. *Journal of the American Chemical Society* **1933,** *55* (11), 4571-4587.
12. Nagarjuna, G.; Hui, J.; Cheng, K. J.; Lichtenstein, T.; Shen, M.; Moore, J. S.; Rodríguez-López, J., Impact of Redox-Active Polymer Molecular Weight on the Electrochemical Properties and Transport Across Porous Separators in Nonaqueous Solvents. *Journal of the American Chemical Society* **2014,** *136* (46), 16309-16316.
13. Ahmad, M.; Abdul Raman, A. A.; Basirun, W. J.; Bhargava, S. K., Treatment of textile effluent containing recalcitrant dyes using MOF derived Fe-ZSM-5 heterogeneous catalyst. *RSC Advances* **2016,** *6* (56), 51078-51088.
14. Collomb, M.-N.; Deronzier, A.; Gorgy, K.; Leprêtre, J.-C.; Pe'caut, J., Electrochemical properties of [FeIII(L)2Cl2][PF6] and [Fe2III,IIIO(L)4Cl2][PF6]2 [L=2,2'-bipyridine (bpy) and 4,4'-dimethyl-2,2'-bipyridine (dmbpy)]. Crystal structures of the dmbpy derivatives. *New Journal of Chemistry* **1999,** *23* (7), 785-790.

15. Huang, Y.; Moret, M.-E.; Klein Gebbink, R. J. M.; Lutz, M., Crystallographic Space Group Choice and Its Chemical Consequences: Revised Crystal Structure of [Fe(phen)2Cl2]NO3. *European Journal of Inorganic Chemistry* **2013,** *2013* (13), 2467-2469.
16. Figgis, B.; Patrick, J.; Reynolds, P.; Skelton, B.; White, A.; Healy, P., Structural studies in the iron(III)/chloride-diimine system. Ionic derivatives of stoichiometry $FeCl_3(phen,bpy)_{1,1.5}$. J Australian Journal of Chemistry. **1983,** *36* (10), 2043-2055.